Phase and cell Imbalance compensation in grid connected imbalanced Photovoltaic systems

Chandrasekhar.s[#1], Y.Rajesh babu*[2]
[#]*Narasaraopeta engineering college, India*
[1]209chandra@gmail.com
[*]*Narasaraopeta engineering college, India*
[2]yrajesh@gmail.com

***Abstract*— Due to the depletion of non-renewable energy resources trend towards the growth of photovoltaic systems is increasing. This photovoltaic power generation is increased to the level of grid interfacing. To connect this large scale power to the grid multistring topology is used where large numbers of PV cells are connected in series. A cascaded H-bridge Multilevel Inverter is used in order to get the 7-level output from the input DC supply. Boost chopper is used here to get required voltage from the strings.**

Even though we are using the multistring topology we still have some imbalance problems among the cells of the same phases and among the different phases of the system. So these imbalances will not be allowed by the grid standards because each phase is getting the different power. In this paper a per phase and per cell imbalance compensating techniques are used to overcome the imbalance problem. Mat lab/Simulink is used to solve the problems raised in the system.

***Keywords* — Multistring, multilevel, photovoltaic and H-bridge.**

I. INTRODUCTION

Now a day's solar photovoltaic energy conversion systems are the fastest growing renewable energy source in the world since last decade. Even though there is increase in the photovoltaic energy systems the problems involved with the PV systems are increasing [1]. It has increased at an annual average of 60% per year. (7 GW installed in 2009 only, with a total of 21 GW installed capacity worldwide) [2]. Large-scale PV utility plants range from 200 kW up to almost 100 MW (the largest is of 97 MW in Sarnia, ON, Canada). Currently there are more than 150 utility-scale PV plants over 10 MW [3]. There is a clear global trend to increase the capacity and quantity of utility-scale PV plants.

Currently large-scale PV plants are interfaced to the grids by two types of topologies: The centralized topology and the multistring topology [3].In the centralized topology large number of PV modules are connected in series to get the desired PV string voltage. Several of these strings are connected in parallel to reach the required power level of the PV system. Obtained dc power is connected to the grid by a centralized grid-tied inverter which is a three-phase 2-level voltage source inverter. Isolation is usually provided by a low frequency transformer at the ac side. The advantage of this topology is simple in structure and control (only one converter) and reduced cost. The main disadvantage of this topology is the lower power output due to a single (MPPT) maximum power point tracking for the whole plant, which is affected by module mismatch and partial shading. On the other hand, the multistring concept [4] also uses centralized grid tied inverter, but has a distributed dc-bus in which each string is connected through a chopper. Commonly these are boost choppers, if isolation is provided at the ac side, or a high frequency isolated dc-dc converters (like a fly back or push-pull converter), if isolation is required at dc side [5]. The main advantage of the multistring topology is the increased modularity, allowing to combine different types of modules and even choppers. It also separates the grid converter control from the PV string control, which gives independent MPPT tracking of each string, increasing the power output. The main disadvantage of this topology is the higher cost and complexity of having additional power converters, sensors, and control systems. But the higher conversion efficiency is a superior advantage in long term operation; hence it is considered the state of the art topology today.

Both configurations use the centralized inverter at low voltage (690V), with the given current limitations of semiconductors, allowing a power rating up to 0.7 MW without paralleling converters. This is the main problem for large scale PV plants (megawatt range), where several centralized topologies are needed to interface the power to the grid. The converters can be used as separate centralized topologies dividing the PV plant in subsystems, or connected in parallel as a single one to handle all the power of the PV plant.

The trend of megawatt range PV plants will demand higher power ratings for the central grid tied converter, and traditional two level voltage source converters (2L-VSC) topologies will not be able to fulfill power rating, power quality and efficiency requirements. Moreover, more demanding grid codes could apply to these systems as happens today with wind energy conversion systems [6], pushing further the limits of the 2L-VSC. The use of several 2-level converters also means more power electronics, control systems, sensors, filters, size and cost compared to using a single medium-voltage high-power converter.

Medium voltage converters have been proposed recently for grid connected PV systems [7]–[15]. Most of these proposals are based on the 3-level NPC multilevel converter, and the

single-phase cascaded H-bridge multilevel converter. The NPC topology can be commercially found up to several tens of megawatt (up to 40MVA) and typically connected to 3.3kV and 4.16kV type of grids [16]. To fully use the power rating of an NPC converter too many modules are needed to connect in series to reach the medium voltage and several more in Parallel to reach desired power levels. This issue comes back to the same problem of the centralized topology. An improvement has been made with an NPC multistring approach [15], where the dc-dc stage can help boosting the voltage reducing the number of modules in series. In addition parallel connection is performed with individual strings and their dc-dc converters with all the advantages of the multistring concept. Cascaded H-Bride structure has lot of uses: it provides more dc-links to them PV strings are connected, each one with independent maximum power point, and it easily reaches medium voltage. Even though each H-bridge cell has its independent PV system with its own power point, still there is power imbalance between the cells. If this imbalance is not taken into consideration in the control system, the dc-link voltages will change. The dc-link voltage imbalance reduces the power quality introducing voltage distortion at the grid side, and more importantly, gives problem for the converter if voltage limits of the capacitors changes.

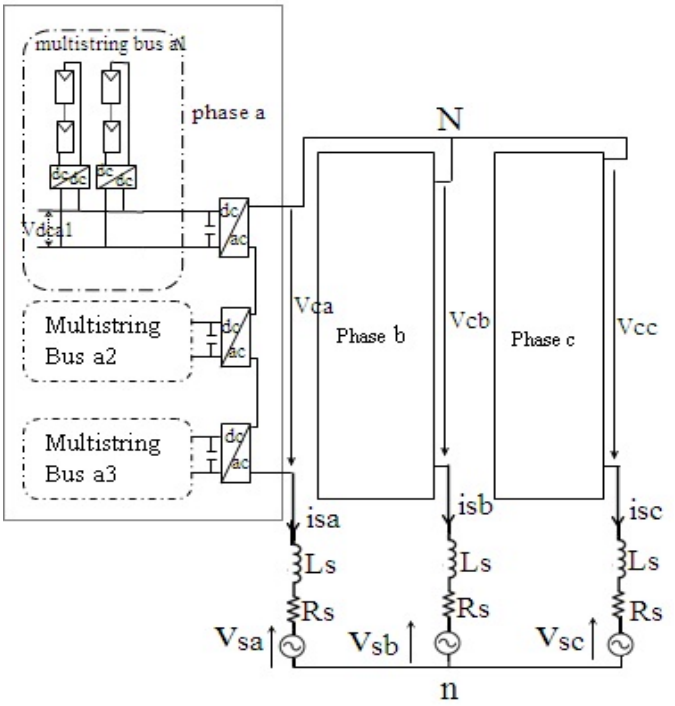

Fig. 1. Proposed cascaded H-bridge multistring PV system configuration.

However, the three-phase CHB introduces an additional challenge, which is the imbalance between the three phases, since each cell has its own MPPT. It leads to unbalanced currents, which will not be allowed by grid codes.

Compensation techniques for three-phase CHB converter are proposed to deal with this imbalance, by shifting the neutral of the reference voltages so that the currents are balanced. This is achieved through a weighted zero sequence injection, in which each phase voltage reference is inversely compensated according to the respective imbalance ratio. This acts as a feed forward mechanism correcting the undesired behavior. In addition, to increase the power capacity of the total PV system, the multistring concept is introduced to each dc-link of the CHB. This enables to connect several strings in parallel to each H-bridge cell, each with its independent maximum power point. By this way, very large PV plants can be connected into a single CHB, with the benefits of improved power quality, more efficiency, single control system, one set of sensors, one line filter, etc. In this paper the proposed configuration and control system is simulated for a three-phase seven-level cascaded H-bridge inverter, so that it reaches voltage of 3.3kV for the given limits. Configuration and control methods can be directly extended for cascaded H-bride cells of any number of levels to get any level of voltage [16].

II. PROPOSED TOPOLOGY DESCRIPTION

Proposed three-phase cascaded H-bride multilevel multistring topology for a PV system is shown in Fig. 1. The circuit is contains three parts the H-bridge power cells of the cascaded H-bridge structure, the PV strings, and the dc-dc converters (boost chopper is used here). Here only one phase is given in detail due to space limitations. Generally used cascaded H-bridges are of three cells per phase (k = 3) to reach 3.3kV voltage level. The converter ac voltages (v_{ca}, v_{cb} and v_{cc}) are made of the sum of the cell output ac voltages and are usually modulated using Phase-Shifted PWM (PS-PWM) to ensure even cell usage [17]. Each cell is modulated with unipolar PWM where the carrier signals are shifted between cells in $¼=k$ rad to produce the multilevel stepped voltage waveform and optimize power quality. It is common to use low switching frequencies due to the power rating of the system, semiconductor limits, efficiency and heat dissipation requirements. Typical carrier signals for each cell (hence average device switching frequency) are of 500Hz, which lead to 1kHz cell output equivalent frequency (due to unipolar PWM) and to kHz equivalent total converter output switching frequency due to the multiplicative effect of the phase-shifts of the carriers among cells. This is why the CHB topology produces lower losses compared to general 2-level converters paralleled to reach required power rating, operating at higher switching frequencies to reach same power quality. In addition, the cascaded H-bridge reaches medium voltage, for which no step up transformer is required.

Photovoltaic strings are composed of the series connection of several PV modules, to reach the voltage level close to the dc-link voltage of one cell of the cascaded H-bridge converter. The number of modules per PV string can be different, they can be of different type and connected through different choppers as long as the chopper is capable to boost the voltage up to the DC-link voltage level. Several PV strings can be

connected to each dc-bus up to the power rating capacity by each cell. Although the strings are connected in parallel to the dc-bus, they have each independent maximum power point tracking because of the boost chopper. For this reason the multistring system is very flexible and modular. The control technique proposed in this paper is able to deal with uneven power distribution among the cells and hence it is technically feasible to have different installed capacity in each dc-bus. Nevertheless, it is desirable to design the system as balanced as possible and leave the imbalances to mismatch among modules, partial shading and even disconnection of a complete string per dc-bus. In this way the proper operation and performance of the overall system can be extended for a greater range.

The choppers can be of different type. The boost converter is one of the most commonly used where systems without isolation are permitted or where ac side isolation is used. In case of the CHB topology it is recommended to use dc-side isolation, so each string can be grounded to avoid hazard conditions produced by parasitic capacitances of the PV modules. In this work, the main contribution is the analysis and control of the power imbalances of the grid tied converter, and therefore less detail will be given on the dc-dc stage control and topology. For sake of simplicity boost chopper is considered in this work.

III. PROPOSED CONTROL METHOD

In this control method two control loops are used to control the multistring topology: one for the CHB inverter which controls the dc-link voltages and grid currents and the other for the boost chopper which is used to control the PV string voltage and adjust it to a desired reference given by the MPPT algorithm. Since the aim of this paper is not a contribution in relation to the dc-dc stage control, classic cascaded current and voltage loops are considered along with the well known perturb and observe (P&O) algorithm [18], [19]. Sections described below explain the control method and power imbalance compensation technique for the centralized CHB converter.

A. Voltage oriented control

The Two most important control methods considered as main-stream solution for grid tied converters are Voltage Oriented Control (VOC), and Direct Power Control (DPC) [20]. Improved versions of both methods based on the virtual flux concept have been also proposed. In this work the VOC method is considered, mainly because it has a modulation stage embedded in the loop (DPC does not use modulation), which makes dealing with the power imbalance a more approachable task, particularly since it is a multilevel converter.

Voltage oriented control scheme block diagram is shown in Fig. 2. Just like general VOC, there is an outer voltage control loop with an embedded inner current control loop. The outer loop controls the dc-link voltage, and since the CHB has several dc-links, an average of them is controlled. In this way the total active power needed to control all the dc-link voltages is computed. The distribution of that active power among the different cells is later carried out in the modulation stage due to the per-phase and per-cell balancing mechanisms. The active power reference given by the voltage loop is proportional to the i_{sd} current component, while the reactive power is proportional to the i_{sq} component. The reactive power reference is usually set to zero, although it can be controlled at different values if required.

Both currents are regulated with PI controllers that give the converter reference voltage, which is then converted from *dq* reference frame to three-phase voltage references. The orientation of the *dq* transformation, or synchronization, is performed through a PLL voltage reference given by the current loop is then modulated using phase-shifted PWM. Note that in order to properly control the dc-link voltages of each cell and compensate the inherent power imbalances introduced by the different PV strings; the modulation stage needs to be modified to address these issues. The problem description and solution for the power imbalance is discussed in the preceding topics.

B. Power Imbalance Problem Description

Generated power by the photovoltaic module depends on two parameters: solar radiation and temperature falling on the module. The maximum power point will depend on these two operating conditions which may vary slightly between adjacent modules, but can be quite different between several sectors of large PV plants due to partial shading and module mismatch. Because of this it is very unlikely to have identical

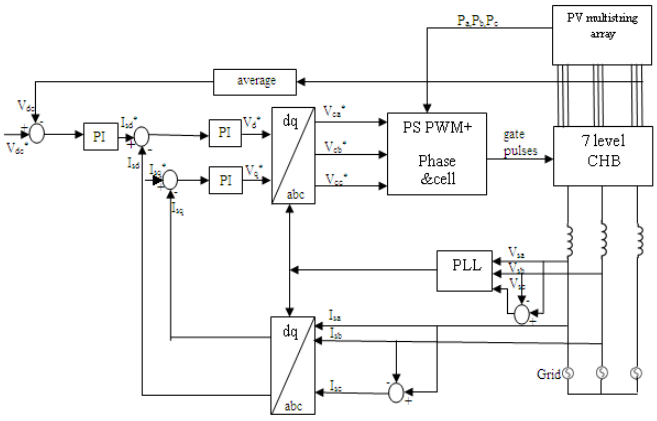

Fig.2. Voltage oriented control diagram with imbalance compensation for proposed topology.

power delivered by each PV string to the power cells of the CHB causing power imbalance among them. Moreover, strings of different size, or interfaced with different dc-dc converters and control systems may further add to the imbalance.

Per-cell imbalance and per phase imbalance are the two types of power imbalances. The first is the power imbalance between the cells of one phase. This means for example that the power processed by each H-bridge of phase *a* are not equal (P_{a1} 6= P_{a2} 6= P_{a3} for a three-cell CHB). The second is the

difference of total power processed: by each phase of the converter ($P_a \neq P_b \neq P_c$). These two type of imbalance affect the control of the CHB converter in two different ways: the per-cell imbalance affects the CHB in two ways : the per-cell imbalance affects the dc-link control loop making the dc-link voltages from one phase to drift from the reference value, which causes distortion and may harm the converter; the per-phase imbalance affects the current control loop making the grid current unbalanced among each other. The fact that VOC returns a single balanced voltage reference, means that if the power is different among the cells the currents must be imbalanced.

C. power imbalance compensation method

The imbalance generated in the system will be compensated by using two compensating techniques: first the per phase imbalance is generating a new reference voltage for each phase, and later the per cell imbalance is compensated generating new reference voltage for each H-bridge cell of the CHB converter.

1) Per phase imbalance compensation: as the voltage oriented control generates the same voltage reference amplitude for each phase, if the power is unbalanced the resulting currents will be unbalanced. The idea then us to unbalance the voltage reference in an inverse way, proportional to power imbalance, so that the resulting currents are balanced and fulfill grid code standards. This can also be seen as a sort of feed forward compensation.

The voltage equations from the power circuit shown in Fig.1 are as follows

$$V_{ca} + V_{Nn} - R_s I_{sa} - L_s \frac{di_{sa}}{dt} - V_{sa} = 0 \quad (1)$$

$$V_{cb} + V_{Nn} - R_s I_{sb} - L_s \frac{di_{sb}}{dt} - V_{sb} = 0 \quad (2)$$

$$V_{cc} + V_{Nn} - R_s I_{sc} - L_s \frac{di_{sc}}{dt} - V_{sc} = 0 \quad (3)$$

Here the grid currents depend for some part on the common mode voltage *VNn*, revealing that common voltage to the three phases can affect the currents. This is an important characteristic because it shows that is possible to balance the currents by moving the neutral point of the converter in a way that the phase voltages are unbalanced inversely proportional to the power unbalance of the converter. This can be easily achieved by calculating the imbalance ratio r_i ($i = a; b; c$) for each cell given by

$$r_a = \frac{P_{av}}{P_a}, \quad r_b = \frac{P_{av}}{P_b}, \quad r_c = \frac{P_{av}}{P_c} \quad (4)$$

Where, P_i ($i = a; b; c$) is the power of each phase and P_{av} is the average power given by

$$P_{av} = \frac{P_a + P_b + P_c}{3} \quad (5)$$

The unbalance ratios are multiplied to the corresponding voltage reference (Vca*,Vcb*,Vcc*) in per unit, which weights or compensates the amplitude of the references according to the unbalance. Then a min-max zero sequence voltage V0 of this weighted reference is given by the equations (6) which gives the value which is useful for further

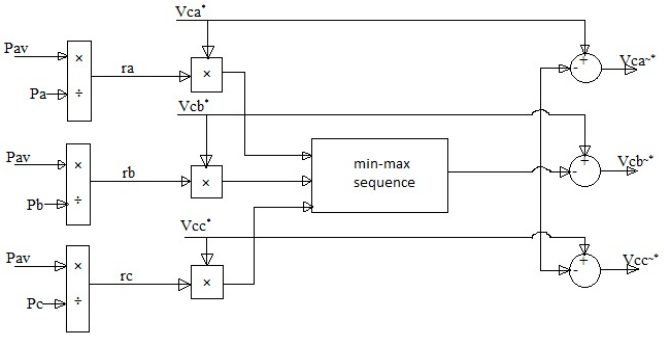

Fig. 3. Proposed phase power imbalance compensation min-max injection block diagram.

$$V_0 = \frac{\max(r_a V_{ca}^*, r_b V_{cb}^*, r_c V_{cc}^*)}{2} + \frac{\min(r_a V_{ca}^*, r_b V_{cb}^*, r_c V_{cc}^*)}{2} \quad (6)$$

and injected to each reference to introduce the corresponding neutral shift. This originates the compensated phase reference voltages

$$V^{\approx *}_{ca} = V^*_{ca} - V_0, V^{\approx *}_{cb} = V^*_{cb} - V_0, V^{\approx *}_{cc} = V^*_{cc} - V_0 \quad (7)$$

The block diagram that performs this simple compensation is given in Fig.3.Most important advantage of balancing the currents in this way is that there is no need to implement more sensors because the powers are already available as they are needed to get for the maximum power point tracking algorithm of the chopping stage, and more over the computational cost is really low, since it consists of a ratio calculation and zero sequence injection, which is usually included.

In order to know more about the operation, a best example of the original references, the weighted references, the min-max zero sequence and the compensated references for an imbalance in phase *a* are given in Fig. 4(a),(b) and (c) respectively. Fig. 4d shows the compensated references in case no unbalance is present, which corresponds to traditional min-max sequence injection.

2) Per-cell imbalance compensation: Even though the compensation of the per phase imbalance is done still there is a chance that the power delivered to the different cells of one phase of the converter is also unbalanced. The modulation is done using phase-shifted PWM[17]) and therefore the compensated voltage reference given by the VOC loop is the same for all the cells. The carrier signals are shifted to produce the multilevel stepped waveform, but essentially will impose the same average usage of the cells drawing similar

average current from each one. In presence of unbalance this will cause voltage drift of the dc-links causing distortion in the converter voltage and possible damage of the power cells. The cell imbalance is seen in the past for single phase cascaded H-bridge PV systems. The same approach used in [14] is considered in this work, and therefore will not be addressed in full detail.

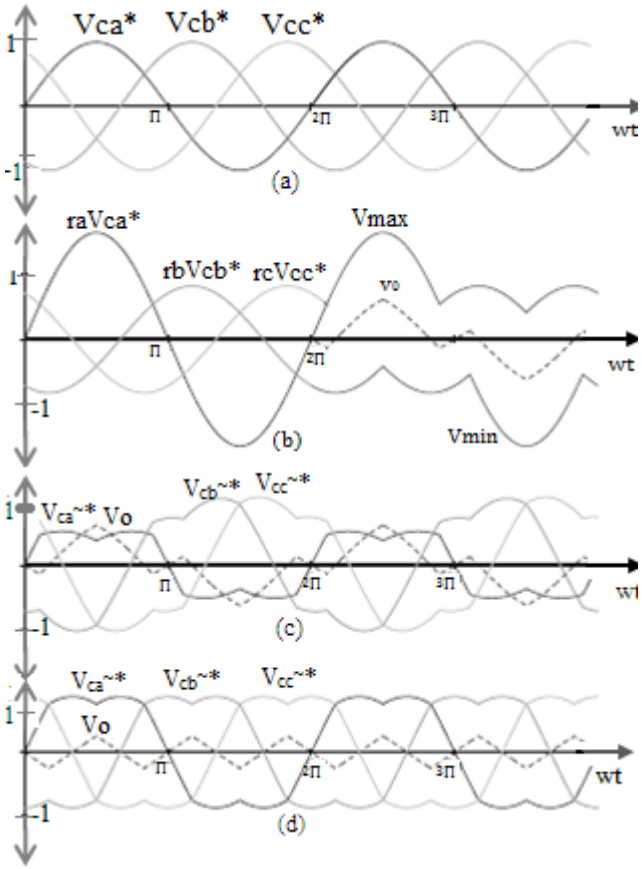

Fig. 4. An example of phase *a* imbalance reference compensation: a) three-phase converter reference voltages, b) Imbalance compensated reference voltages, c) Imbalance compensated reference voltages with min-max sequence injection, d) Particular case whit no phase imbalance (traditional min-max).

The idea behind the balancing mechanism is to distribute the usage of the cells of one phase in the same proportion of the imbalance by adjusting (redistributing) the on and off times given by the PWM strategy. In this way, more or less

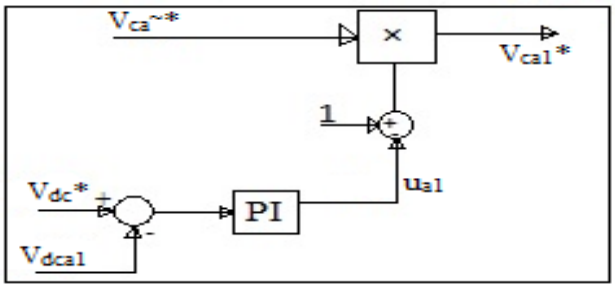

Fig. 5. Per cell power imbalance compensation for PS-PWM only power cell *a*1 given as example.

active power is drawn by the cell according to the imbalance experimented by the system. Fig. 5 shows how the per cell imbalance is balanced. Voltage error (v_{dc}^{*} - v_{dc}^{a1}) between the DC cells is regulated with a PI controller, whose output is used to adjust the amplitude of the per unit reference signal. In this way the amplitude of the references used for each cell are modified proportionally to the error of their respective dc-link voltages. So the on and off times are changed and the balance is achieved by changing switch timings.

IV.RESULTS

The simulation is done for a three-phase 7-level cascaded H-bridge with three cells per phase at voltage rating of 3.3kV. Each dc-link is controlled to 1150V. The PV module modeled at rated power output of 235 W and 30V rated voltage at 25^{o}C with a solar radiation of 1kW/m^{2}. Considering the dc-link voltage and the module rated output voltage a total of 30 PV modules in series are considered. In addition to have a more realistic simulation in terms of power output, 20 strings, each with individual dc-dc stage have been paralleled per power cell. This makes a total of 5400 modules rated at total of 1.26MW. Mat lab/simulink has been used for the simulation. All the system and simulation parameters are shown in Table I the dynamic and steady state performance of the proposed imbalance control method is done by doing two step changes to the radiation level. All power cells of the converter start at rated temperature (25^{o}C) and radiation (1kW/m^{2}). At *t*=0.5s a step change to the radiation of the strings connected to cell *a*2 and *a*3 is performed to force a per cell imbalance. Radiation is lowered to 0.75pu and 0.5pu respectively.

This is an extremely high imbalance of up to 50% compared to cell *a*1. Note that this imbalance also implies a per phase imbalance since, phase *a* of the converter will be operating at lower power than phase *b* and *c*. In addition, a harder per phase imbalance is forced at *t*=0.6s by reducing the radiation to all the strings connected to phase *c* in 50%.Phase *b* is the only one not modified throughout the experiment. The simulation results for the dynamic changes described earlier are illustrated in Fig. 6–8. The effect of the power imbalances can be better appreciated in the change introduced to the voltage reference signals, shown in Fig. 6 In Fig. 6a the phase compensated voltage references are illustrated. It can be clearly appreciated that during balanced operation up to 0.5s no compensation is per-formed obtaining the traditional min-max injection reference waveform studied earlier in Fig. 4d. From 0.5s to 0.6s there is a small per phase imbalance due to the changes introduced to phase *a*. This can be seen in Fig. 6a, where the weighted min-max compensation becomes evident for phases *b* and *c*. The per cell imbalance in phase *a* is noticeable in Fig. 6b where the amplitudes of the references for each cell of phase *a* are modified according to the respective imbalance. Note how the amplitude of reference of cell *a*3 is reduced almost to the half due to the 0.5pu radiation step change. By reducing the voltage reference, the on times are shorter reducing the power drawn from the cell, enabling the dc-link voltage to stay at the desired level. Finally, at *t*=0.6s the per phase imbalance becomes stronger since all the strings of phase *c* have experienced a 50% reduction in

radiation. Note that per-phase and per-cell imbalances are occurring at the same moment after *t*=0.6s. This is not a problem, since both compensations are performed sequentially one after the other allowing to control both type of imbalances.

Total performance of the voltage oriented control can be observed in Fig. 7. The resulting modulated converter output voltage waveforms of the references analyzed previously are

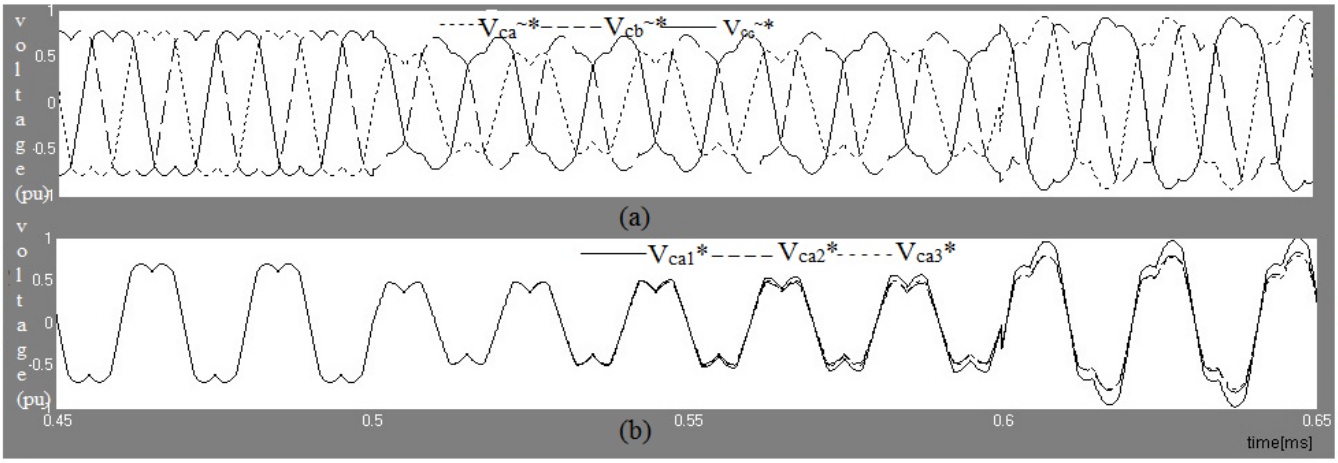

Fig. 6 Converter reference voltages: a) Compensated reference voltages for a phase imbalance in phase c at t = 0:6[s], b) Compensated references for each cell of phase a ($v_{ca}^*{}_1$, $v_{ca}^*{}_2$, $v_{ca}^*{}_3$) with cell imbalance at t = 0:6[s].

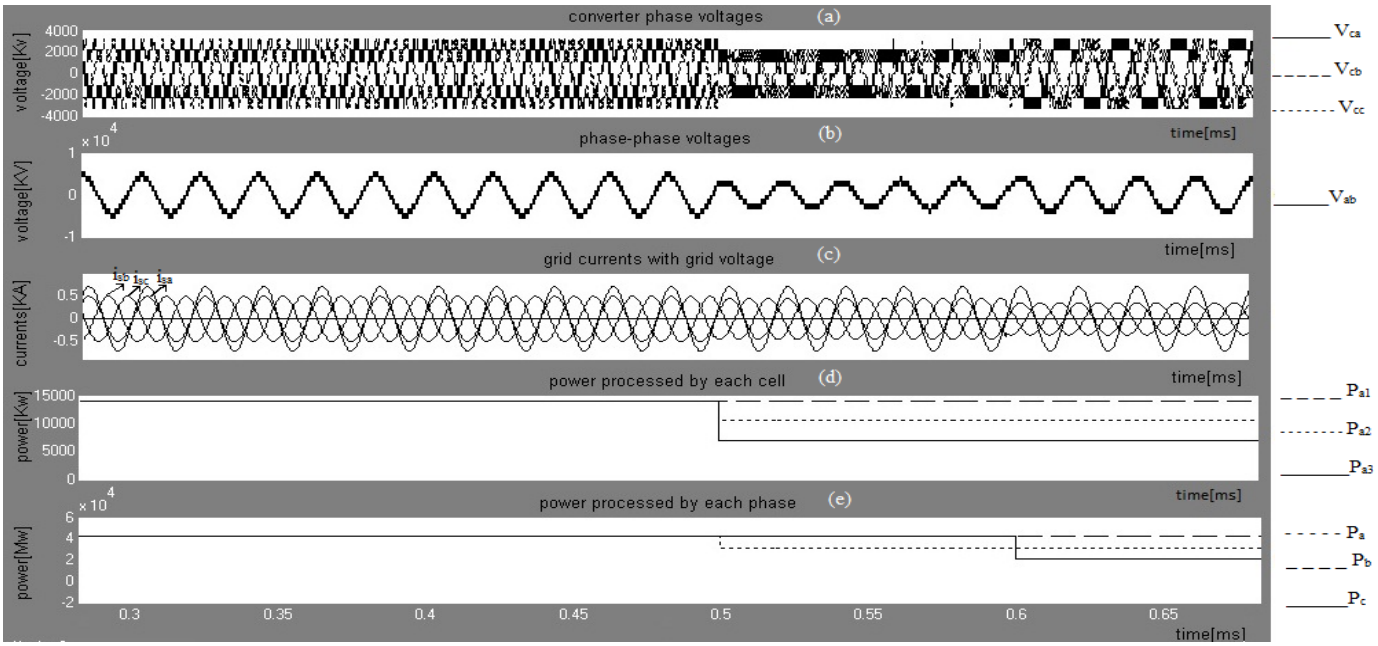

Fig.7 dynamic performance with step cell imbalance in phase a at t=0.5[s] and a step phase imbalance in phase c at t=0.6[s]: (a) converter phase voltages (Vca,Vcb,Vcc), (b) line-line converter voltage(Vab), (c) grid currents(isa,isb,isc) with grid voltage Vsa shown to highlight synchronism, (d) power processed by each cell of phase a(Pa1,Pa2,Pa3), (e) power processed by each phase(Pa,Pb,Pc).

shown in Fig. 7a. The imbalance compensation and min-max sequence can be clearly appreciated in these inverter phase voltages. Since the min-max injection is a zero sequence it should not appear in the line-line voltages, this can be appreciated in Fig. 7b, which appears sinusoidal in shape. The accurate performance of the imbalance compensation can be better appreciated in Fig. 7c, where the three-phase grid currents appear completely balanced, despite the converter phases are operating at different power levels.

The grid phase voltage v_{sa} has been scaled down and plotted together with the currents (dashed line) to show the proper synchronism achieved with the PLL. Power processed by each cell of converter is illustrated in Fig. 7d. Here the effect of the step change in the solar radiation given to cell *a*2 and *a*3 is clearly noticeable. Finally the total powers of each phase of the converter are given in Fig. 7e. Apart from the power reduction at *t*=0.5s of phase a the step change in radiation in phase *c* at *t*=0.6s can also be appreciated. Note that phase *b*

does not experiences significant power changes throughout the experiment, confirming that the different dc-dc stages and multistring PV systems operate independently from each other at their own MPPT[18]. The system proves to keep working with high performance and power quality despite the severe imbalances introduced to the operation of the different cells and phases.

To show the imbalance compensation control method the dc-link voltages of the three cells of each phase are given in Fig. 8. The dynamic behavior of the per-cell imbalance

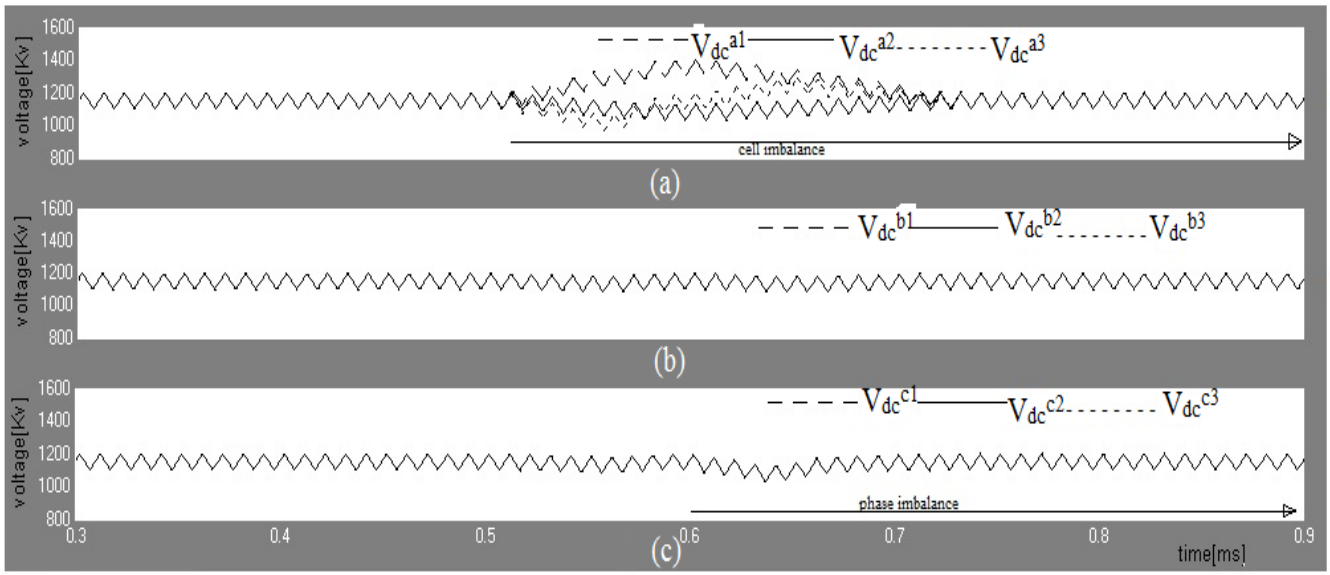

Fig.8. Dc-link voltages with cell imbalance in phase a at t=0.5s and with phase imbalance in phase c at t=0.6s,a) of phases a,b and c.

Table – 1
SIMULATION PARAMETERS

Parameter	Symbol	Value
Line to Line Grid Voltage	vs_{ll}	3:3 kV_{RMS}
Grid Frequency	*fs*	50 Hz
Rated Power	*P*nom	1:2 MW
Rated Current	*i*snom	300 A_{RMS}
Input filter inductance	*Ls*	2 mH
Input filter resistance	*Rs*	0:1 m-
DC-link capacitance	*C*	3700 ¹F
DC-link voltage reference per cell	v_{dc}^*	1150V
Total DC-link voltage per phase	$3v_{dc}^*$	3450V
Device avge. switching freq.	*f*sw	500 Hz
Equivalent output freq. per phase	*f*sw	3000 Hz
No. of strings connected to each dc-bus	*Np*	20
No. of series connected PV modules per string	*Ns*	30
Open circuit voltage of module	*V*oc	37 V
Maximum power voltage of module	*V*pm	30 V
Short circuit current of module	*V*sc	8:6 A
Maximum power current of module	*I*pm	7:84 A

compensation can be appreciated in the dc-link voltages of phase *a* shown in Fig. 8a, from t=0.5s. Although the compensation is achieved compensating the three phases, the impact on the dc-link voltages of phase a and phase b is negligible. In fact, the dc-link voltages of phase b which has not experienced any change in radiation presents very small deviation from the reference due to minimal coupling of variables [20]. Results show that the phase and cell imbalance compensating techniques successfully compensated the imbalance even though there is change in radiation.

V. CONCLUSION

In this paper new medium voltage converter interface for large scale PV energy conversion systems is presented. It is based on a three-phase CHB multilevel multistring topology. The multistring converter structure composed of isolated dc-dc and a grid tied dc-ac converter, effectively decouples the grid side control from the PV string control requirements.

This allows independent MPPT control of each string without affecting the dc-link voltages of each cell. The main challenges related to the configuration are the possible existence of two types of power imbalance: between the power cell of one phase of the converter. These challenges are solved by using two compensating techniques: one is per phse imbalance compensation and another is per-cell imbalance compensation. In the first one it is applied to the reference voltage of each phase by means of power ratio and a min-max zero sequence, and other by adjusting the modulation index of different references of each cell used in the phase shifted modulation of a phase of the converter. The compensation methods can work even under combined power imbalances. The three-phase CHB multistring topology with the given control techniques and imbalance compensation methods can be applied to any kind of system. Advantages are superior power quality of the CHB.

VI.REFERENCES

- S.Rivera, S.Kouro, B.Wu, J.I. Leon, J.Rodrigue, L.G Franquelo "cascaded H-bridge multilevel converter multistring topology for large scale photovoltaic systems".IEEE transactions 978-1-4244-9312-8/11-2011.[1]
- pvresources.com, "Large-scale photovoltaic power plants: ranking,"available at http://www.pvresources.com/en/top50pv.php.[2]
- F. Blaabjerg, Z. Chen, and S. B. Kjaer, "Power electronics as efficient interface in dispersed power generation systems," IEEE Trans. Power

Electron., vol. 19, no. 5, pp. 1184–1194, Sep. 2004.[3]

- M. Meinhardt and G. Cramer, "Multi-string-converter: The next step in evolution of string-converter technology," in in Proc. 9th Eur. Power Electronics and Applications Conf., 2001.[4]
- M. Meinhardt and G. Cramer, "Multi-string-converter: The next step in evolution of string-converter technology," in in Proc. 9th Eur. Power Electronics and Applications Conf., 2001.[5]
- S. B. Kjaer, J. K. Pedersen, and F. Blaabjerg, "A review of single-phase grid-connected inverters for photovoltaic modules," IEEE Trans. Ind. Applicat., vol. 41, no. 5, pp. 1292–1306, Sep./Oct. 2005.[6]
- "Grid code - high and extra high voltage," E.ON Netz Gmbh, April 2006.[7]
- M. Calais and V. G. Agelidis, "Multilevel converters for single-phase grid connected photovoltaic systems-an overview," in Industrial Electronics, 1998. Proceedings. ISIE '98. IEEE International Symposium on, vol. 1, Jul. 7–10, 1998, pp. 224–229.[8]
- S. Busquets-Monge, J. Rocabert, P. Rodriguez, S. Alepuz, and J. Bordonau, "Multilevel Diode-clamped Converter for Photovoltaic Generators With Independent Voltage Control of Each Solar Array," IEEE Trans. Ind. Electron., vol. 55, no. 7, pp. 2713–2723, Jul. 2008.[9]
- J. Selvaraj and N. A. Rahim, "Multilevel Inverter For Grid-connected PV System Employing Digital PI Controller," IEEE Trans. Ind. Electron., vol. 56, no. 1, pp. 149–158, Jan. 2009.[10]
- N. A. Rahim and J. Selvaraj, "Multi-string Five-level Inverter with Novel PWM Control Scheme for PV Application," IEEE Transactions on : Accepted for future publication Industrial Electronics, pp. 1–1, / 2009.[11]
- G. Grandi, C. Rossi, D. Ostojic, and D. Casadei, "A New Multilevel Conversion Structure for Grid-connected PV Applications," IEEE Trans. Ind. Electron., vol. 56, no. 11, pp. 4416–4426, Nov. 2009.[11]
- E. Villanueva, P. Correa, J. Rodriguez, and M. Pacas, "Control of a Single-phase Cascaded H-bridge Multilevel Inverter for Grid-connected Photovoltaic Systems," IEEE Trans. Ind. Electron., vol. 56, no. 11, pp. 4399–4406, Nov. 2009.[12]
- L. Ma, X. Jin, T. Kerekes, M. Liserre, R. Teodorescu, and P. Rodriguez, "The PWM strategies of grid-connected distributed generation active NPC inverters," in Energy Conversion Congress and Exposition, 2009. ECCE. IEEE, Sep. 20–24, 2009, pp. 920–927.[13]
- S. Kouro, A. Moya, E. Villanueva, P. Correa, B. Wu, and J. Rodriguez, "Control of a cascaded h-bridge multilevel converter for grid connection of photovoltaic systems," in 35th Annual Conference of the IEEE Industrial Electronics Society (IECON09), 2009, pp. 1–7.[14]
- S. Kouro, K. Asfaw, R. Goldman, R. Snow, B. Wu, and J. Rodríguez, "Npc multilevel multistring topology for large scale grid connected photovoltaic systems," in 2010 2nd IEEE International Symposium on Power Electronics for Distributed Generation Systems (PEDG 2010), 2010, pp. 400–4005.[15]
- S. Kouro, M. Malinowski, K. Gopakumar, J. Pou, L. G. Franquelo Wu, J. Rodriguez, M. A. Pérez, and J. I. Leon, "Recent advances and industrial applications of multilevel converters," IEEE Trans. Ind. Electron., vol. 57, no. 8, pp. 2553–2580, August 2010.[16]
- D. P. Hohm and M. E. Ropp, "Comparative study of maximum power point tracking algorithms," Progress in Photovoltaics: Research and Applications, vol. 11, no. 1, pp. 47–62, 2003.[17]
- N. Femia, D. Granozio, G. Petrone, G. Spagnuolo, and M. Vitelli, "Predictive & adaptive mppt perturb and observe method," IEEE Transactions on Aerospace and Electronic Systems, vol. 43, no. 3, pp. 934–950, 2007.[19]
- M. Malinowski, M. P. Kazmierkowski, and A. M. Trzynadlowski, "A comparative study of control techniques for pwm rectifiers in ac adjustable speed drives," IEEE Transactions on Power Electronics, vol. 18, no. 6, pp. 1390–1396, November 2003.[20]